EUROPEAN FUSION DEVELOPMENT AGREEMENT

EFDA–JET–CP(01)01-07

F. Meo, M. Brambilla, R. Bilato, J-M. Noterdaeme, C. C. Petty, F. Nguyen,
and EFDA-CSU Garching and Task Force H Contributors

Comparison of FWCD Scenarios on ASDEX-Upgrade, JET, and DIII-D Tokamaks

Comparison of FWCD Scenarios on ASDEX-Upgrade, JET, and DIII-D Tokamaks

F. Meo[1], M. Brambilla[1], R. Bilato[1], J-M. Noterdaeme[1], C. C. Petty[2], F. Nguyen[3], and EFDA-CSU Garching and Task Force H Contributors

[1]*Max-Planck-Institut für Plasmaphysik, EURATOM Association*
[2]*General Atomics*
[3]*CEA - d'Etudes / Département de Recherches sur la Fusion Contrôlée*

Preprint of Paper to be submitted for publication in Proceedings of the
14th APS Topical RF Conference,
(Oxnard, C.A., USA 7-9 May 2001)

ABSTRACT

A detailed quantitative study of the power absorption and predicted current drive, currently using Ehst-Karney parameterisation, will be presented on three tokamaks; ASDEX, DIII-D, and JET. The 2D full wave toroidal code TORIC is used to calculate the FW current drive efficiency weighted over the complete launched spectrum from the antenna. The code can simulate the complex physics of the efficiency and power balance of all three damping mechanisms as a function of plasma parameters and of $n_{||}$. The code takes into account electron Landau damping of both the Fast Wave (FW) and Ion Bernstein waves and cyclotron damping at the fundamental and first harmonic. Results have shown that the current drive efficiency (normalized to the density) is machine dependent. The results have also demonstrated the importance of taking into account the full spectrum.

1. INTRODUCTION

The total current drive will depend on the current drive efficiency and the absorption. The single pass FW absorption $\propto \omega n^{3/2} T_e B^{-3}$ for $v_{phase} \sim v_{thermal}$ and the largest absorption will occur at $v_{phase}/v_{thermal}$ ~0.7 [1], favouring larger n_ϕ. On the other hand, the current drive efficiency, scales as *T/n*, favouring smaller n_ϕ. The paper will present quantitative simulation results of FWCD of three tokamaks, ASDEX-U, JET, and DIII-D taking into account the total predicted launched spectrum associated with the machine antenna and frequency. We will also compare experimentally determined FW current density profile on DIII-D [2].

SIMULATION TOOLS

Two 3D finite element full wave codes are used. Both codes solve the finite Larmor radius (FLR) equations in the ion cyclotron frequency range. They describe the compressional and shear Alfven waves and the lowest ion Bernstein (IB) waves excited by mode conversion. Both include electron Landau damping of IB Waves. FELICE is a full wave code in a slab geometry. The code solves the wave equations over a n spectrum in either the whole plasma with a metallic boundary or with an outward radiation condition at some point in the plasma. The latter procedure helps to investigate single pass absorption. FELICE also contains a self-consistent antenna evaluation section which can calculate (in simple geometry) the power spectra and antenna loading resistance. TORIC [3] solves the FLR equations in an arbitrary toroidal geometry at one n_ϕ. TORIC includes current drive efficiency calculation from the Ehst-Karney parameterisation [4]. The Ehst-Karney parameterisation takes into account toroidal effects such as trapping and assumes that each toroidal wave number drives current independent of each other.

ICRF SYSTEMS AND FWCD SCENARIO:

The ICRF hardware descriptions for the ASDEX-Upgrade [5], JET [6], and DIII-D [7] tokamaks are summarised in Table 1a. The scenarios chosen for each machine are shown in Table 1b. These scenarios minimise absorption of other damping mechanisms and are of practical relevance to experiments. For

ASDEX-U and JET, the fundamental resonance layer of deuterium lies in the plasma periphery on the high field side. For DIII-D, the 2nd harmonic hydrogen resonance layer lies 40cm from the centre on the high field side and the 3rd harmonic hydrogen resonance layer lies 25cm from the centre on the low field side. However, we will assume that the 3 rd harmonic minority damping is negligible.

TABLE 1.a ICRF Hardware

Antenna Description (cm)	**ASDEX-U**	**JET**	**DIII-D**
Tokamak Major Radius	165	296	170
Minor Radius	50	90	60
Number of Straps	2	4	4
Radius of Antenna	53.0	95.5	69.0
Strap width	18.0	15.6	7.49
Gap	20.0	26.4 / 37.4 / 26.4	11.1 / 11.1 / 11.1
Peak $k_{\|}$(π/2 phasing) (m^{-1})	3.6	7.0	9.0
Antenna height	100.0	122.0	38.64

TABLE1b. FWCD Scenario

Frequency (MHz)	30	37	83
B_o	2.9	3.45	2.1
$v_{ph}/v_{thermal}$ (at 6.5 keV)	1.6	1.0	1.5

SIMULATION RESULTS:

A series of TORIC calculations are performed for every mode number covering the predicted launched spectrum associated with the antenna and frequency for different target plasmas. One of the target plasma corresponds to the one in Ref. [2] where the FW current drive density profile was experimentally determined i.e. $n_e(0) = 4.3 \times 10^{19}$ m^{-3}, n_e(edge) = 1.0×10^{19} m^{-3}, $T_e(0) = 6.5$ keV, T_e(edge) = 0.9keV. Figure 1 shows one of the TORIC results of DIII-D as a function of n_ϕ. Fig 1a shows the power spectrum and the single pass absorption (SPA) both calculated from FELICE as a function of n_ϕ. The higher frequency and lower magnetic field of this scenario on DIII-D favours higher SPA compared to ASDEX case (SPA < 8 %) and JET (SPA < 12 %). Fig1b shows the power balance as a function n_ϕ between the minority hydrogen and the electrons. We can see that at lower n_ϕ, where the phase velocity is high, there is less absorption to the electrons. It is important to note that ~20% of the power is absorbed to the minority hydrogen at $n_\phi = 18$ (maximum value for DIII-D antenna) as opposed to 9% when taking into account the whole spectrum. Figure 1c shows the total current drive efficiency as a function of n_ϕ. The total current density weighted over the antenna for each tokamak are shown in figure 2. The current density profile for DIII-D (Fig.2c) agrees very well with the experimentally determined FW current density profile from Ref [2]. For ASDEX-U and JET, the total power to the

fundamental deuterium accounts for less than 3%. Table 2 summarises the results for each machine for different target plasmas. The table shows the total FW current (IFW) at maximum n_ϕ, I_{FW} over the complete spectrum, and the current drive figure of merit (η_{FW}) for each machine. The table highlights the large difference between I_{FW} calculated at the maximum n_ϕ and calculated over complete spectrum. As expected, the I_{FW} scales as *T/n* for each machine. To compare each tokamak, figure 3 plots the current drive figure of merit η_{FW} as a function of maximum T_e. The η_{FW} is defined as $\eta_{FW} = I_{FW}\,\bar{n}_e\,R/P_{FW}$ where I_{FW} is the total FW current, $\bar{n}_e$ is the line average density, P_{FW} is the total absorbed power, and *R* is the major radius.

Table 2.

I_{FW} at max n_ϕ (kA/MW): I_{FW} over total spectrum (kA/MW): η_{FW} (10^{20} A/W/m^2)
($n_e(0) = 4.3 \times 10^{19}$ m^{-3}, $\bar{n}_e = 3.4 \times 10^{19}$ m^{-3})

	ASDEX-U	JET	DIII-D
n_ϕ(max) with π/2 phasing	6	12	18
$T_e(0)$ = 6.5 keV	165 : 52.4 : 0.030	90 : 50.3 : 0.051	137 : 74.0 : 0.042
$T_e(0)$ = 8.25 keV	126 : 63.4 : 0.037	105 : 62.0 : 0.063	153 : 84.1 : 0.050
$T_e(0)$ =10.0 keV	175 : 76.0 : 0.044	126 : 73.5 : 0.075	176 : 107 : 0.061

Figure 3 also contains experimentally determined η_{FW} on DIII-D [2] and Tore Supra [8]. The TORIC predicted values for DIII-D follow the same dependence with experiments. Even though we also see the same linear dependence of T_e for the TORIC predictions for JET and ASDEX-U, the η_{FW} has a constant portion (offset) which is machine and antenna dependant. Future studies will investigate the dependence on the plasma profile, tokamak aspect ratio, poloidal antenna coverage, the q-profile, and the directivity and phase velocity of the launched spectrum.

REFERENCES

[1]. M. Porkolab, Proceedings Stix Symposium May 4, 1992

[2]. C.C. Petty, F.W. Baity, J.S. deGrassie et al, Nuclear Fusion **39** (1999) 10

[3]. Brambilla, Plasma Phys. Controlled Fusion **41** (1999) 1

[4]. D. A. Ehst and C. F. F. Karney, Nucl. Fusion **31** (1991) 1933

[5]. J. M. Noterdaeme, et al Fusion Engineering and Design **24** (1994) 65-74

[6]. A.Kaye et al., Fusion Engineering and Design, **24**(1994) 1-21

[7]. R.H.Goulding, et al., in Proceedings of the 9th Topical Conference on Radio Frequency Power in Plasmas (Charleston, South Carolina, 1991)

[8]. A. Becoulet, Plasma Phys. Control Fusion **38**, (1996)

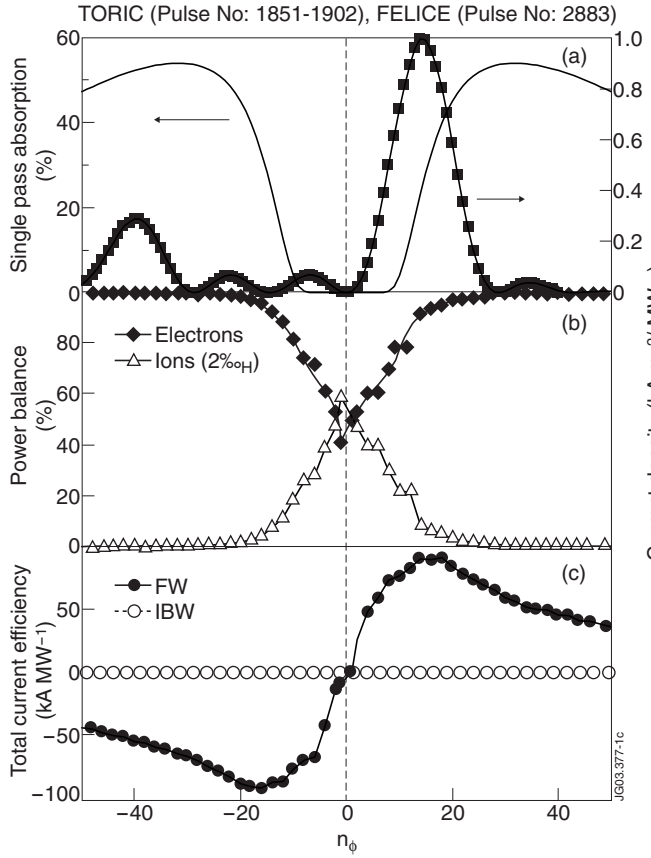

Figure 1: DIII-D FWCD Scenario (a) Power spectra and the single pass absorption as a function of n_ϕ. (b) Power balance between 2nd harmonic Hydrogen and electrons. (c) Total current drive efficiency as a function of n_ϕ.

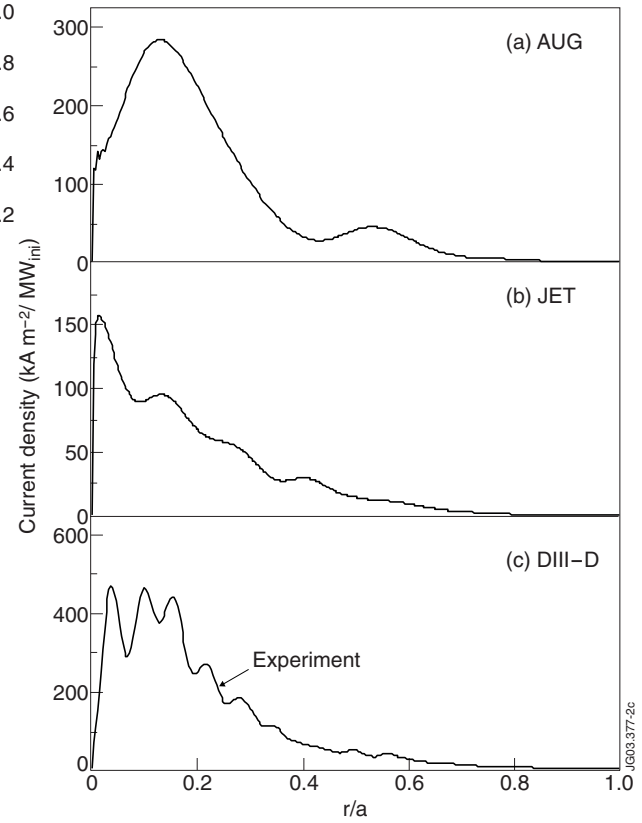

Figure 2: FWCD profile for each tokamak and the experimentally determined FW current profile from Ref. [2]

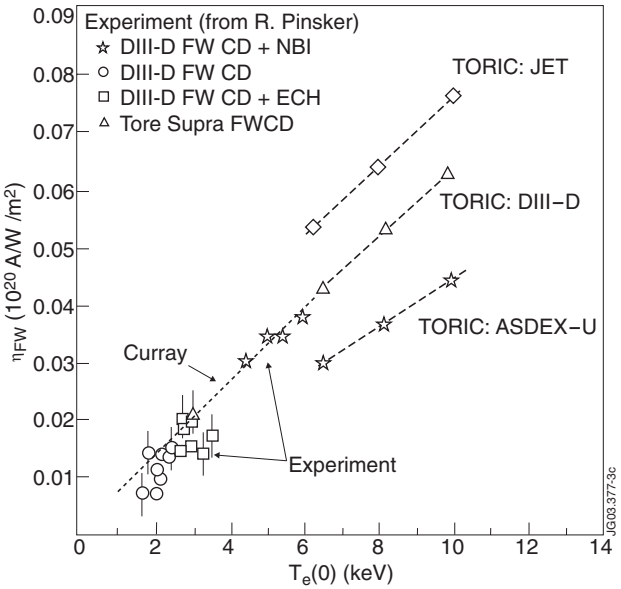

Figure 3: Experimental and TORIC predicted values for the FW current drive figure of merit.